AGU PUBLICATIONS

JGR

Journal of Geophysical Research: Biogeosciences

RESEARCH ARTICLE
10.1002/2017JG003989

**Key Points:**
- Summer temperatures on the eastern slope of the Northern Patagonian Andes were +0.6°C warmer during the 20th than the 19th century
- The temperature signal is better recorded in cellulose $\delta^{13}C$ values than in tree growth of *F. cupressoides*
- The recent increase in tree growth on the eastern slope of the Northern Patagonian Andes is likely due to the $CO_2$ fertilization effect

**Supporting Information:**
- Supporting Information S1

**Correspondence to:**
A. Lavergne,
a.lavergne@imperial.ac.uk

**Citation:**
Lavergne, A., Daux, V., Pierre, M., Stievenard, M., Srur, A. M., & Villalba, R. (2018). Past summer temperatures inferred from dendrochronological records of *Fitzroya cupressoides* on the eastern slope of the northern Patagonian Andes. *Journal of Geophysical Research: Biogeosciences*, *123*, 32–45. https://doi.org/10.1002/2017JG003989

Received 12 JUN 2017
Accepted 10 DEC 2017
Accepted article online 18 DEC 2017
Published online 9 JAN 2018



# Past Summer Temperatures Inferred From Dendrochronological Records of *Fitzroya cupressoides* on the Eastern Slope of the Northern Patagonian Andes

**Aliénor Lavergne[1,2], Valérie Daux[1], Monique Pierre[1], Michel Stievenard[1], Ana Marina Srur[3], and Ricardo Villalba[3]**

[1]Laboratoire des Sciences du Climat et de l'Environnement, CEA-CNRS-UVSQ, Gif-sur-Yvette, France, [2]Department of Life Science, Imperial College London, Ascot, UK, [3]Instituto Argentino de Nivología, Glaciología y Ciencias Ambientales, IANIGLA-CONICET, Mendoza, Argentina

**Abstract** Estimating summer temperature fluctuations over long timescales in southern South America is essential for better understanding the past climate variations in the Southern Hemisphere. Here we developed robust 212 year long basal area increment (BAI) and $\delta^{13}C$ chronologies from living temperature-sensitive *Fitzroya cupressoides* on the eastern slope of the northern Patagonian Andes (41°S). After removing the increasing trend from the growth records likely due to the $CO_2$ fertilization effect, we tested the potential to reconstruct past summer temperature variations using BAI and $\delta^{13}C$ as predictors. The reconstruction based on $\delta^{13}C$ records has the strongest predictive skills and explains as much as 62% of the total variance in instrumental summer temperature ($n = 81$, $p < 0.001$). The temperature signal recorded in tree-ring growth is not substantially different to that present in $\delta^{13}C$ and consequently does not provide additional information to improve the regression models. Our $\delta^{13}C$-based reconstruction shows cold summer temperatures in the second part of the 19th century and in the mid-20th century followed by a warmer period. Notably, the 20th and the early 21st centuries were warmer (+0.6°C) than the 19th century. Reconstructed summer temperature variations are modulated by low-latitude (El Niño–Southern Oscillation) and high-latitude (Southern Annular Mode) climate forcings. Our reconstruction based on $\delta^{13}C$ agrees well with previous ring width based temperature reconstructions in the region and comparatively enhances the low-frequency variations in the records. The present study provides the first reconstruction of summer temperature in South America south of 40°S for the period 1800–2011 entirely based on isotopic records.

**Plain Language Summary** The Southern Hemisphere, and particularly southern South America, are very under-represented in global climate reconstructions due to a lack of robust paleoclimatic data. Here, we reconstruct summer temperature variations on the eastern slope of the Andes in north Patagonia over the last two centuries using tree rings of one of the longest-living species from South America, Fitzroya cupressoides. This reconstruction highlights that the 20th and 21st centuries were warmer (+ 0.6°C) than the 19th century. Our work thus contributes to improve the assessment of the intensity of current climate changes in remote regions from the Southern Hemisphere.

## 1. Introduction

Several studies provided regional to hemispheric syntheses of the Earth's climate history over the past 2,000 years (e.g., Gennaretti et al., 2017; Labuhn et al., 2016; Neukom et al., 2014). Most of them have been focused on the Northern Hemisphere, which has a dense network of paleoclimatic records (Ahmed et al., 2013; Intergovernmental Panel on Climate Change, 2013; Wilson et al., 2016). Substantial efforts have been made over the last decades to fill in the gap in the Southern Hemisphere (SH) by developing millennial-scale climate reconstructions (Boninsegna et al., 2009). However, there is still a need for developing more climate proxies from the SH to improve our understanding of the long-term stability and low-frequency variations of temperature and precipitation beyond the instrumental period.

The north–south extension of the South American forests along the Andean Cordillera provides a unique opportunity to explore the climatic signal recorded in tree rings of native species from tropical to subantarctic regions (Boninsegna et al., 2009; Villalba et al., 2009). Tree rings, which provide precisely dated and annually

resolved records, have been used for documenting past summer temperature variations, in particular, in the temperate regions of southern South America (Lara & Villalba, 1993; Villalba, 1990; Villalba et al., 2003). *Fitzroya cupressoides*, which grows in temperate wet areas in Northern Patagonia (Lara & Villalba, 1993, 1994), may be the most interesting species for long-term climate reconstructions in this area because of its remarkable longevity. Whereas its growth, evaluated by tree ring width measurements, is sensitive to summer temperature conditions prevailing during the previous growing season (Lara & Villalba, 1993, 1994; Neira & Lara, 2000; Villalba, 1990), oxygen and carbon isotope values of tree rings ($\delta^{18}O$ and $\delta^{13}C$) record temperature variations during the current growing season (Lavergne et al., 2016, 2017). Thus, the exploitation of *F. cupressoides* tree ring proxies (ring width, $\delta^{18}O$, and $\delta^{13}C$) will likely contribute to increase the quality of the SH temperature reconstructions over the last millennia.

The temporal stability of the relationship between proxies and climate targets is crucial for reconstructing past variations faithfully (Fritts, 1976). However, a number of tree ring studies have reported an apparent decoupling between relative tree growth and concurrent temperature trends in recent decades at several high-altitude, high-latitude forests in the Northern Hemisphere where temperature has historically controlled tree growth (e.g., Büntgen et al., 2012; Esper et al., 2010). The instability of the relationship, also called divergence, suggests that the dominant environmental drivers of tree growth have changed in recent decades (D'Arrigo et al., 2008). However, the origin of the phenomenon is still debated since much of the divergence could arise from diverse effects including, among others, the statistical techniques used to standardize the tree ring width chronologies (Melvin & Briffa, 2008, 2014). In contrast to ring width derived records, few isotopic studies documented such time-dependent relations between stable isotope chronologies and climate (Daux et al., 2011; Hilasvuori et al., 2009; Naulier et al., 2015; Reynolds-Henne et al., 2007; Seftigen et al., 2011; Young et al., 2011). However, some of them highlighted divergences between $\delta^{13}C$ and summer temperature series over the last decades. Several physical–biological causes have been hypothesized for the divergence: (1) the earlier start of the growing season and the increase of moisture stress with increasing temperature (Hilasvuori et al., 2009; Reynolds-Henne et al., 2007; Seftigen et al., 2011); (2) the uptake of deeper source water in soils during the growing season (Daux et al., 2011); and/or (3) the increase of water uptake from snowmelt due to longer growing seasons (Naulier et al., 2015). These findings question the uniformitarian assumption underlying paleoclimatic reconstructions since statistical tree ring based models calibrated on climate measurements can underestimate or overestimate past climate variations.

*F. cupressoides* growth was consistently related to summer temperature variations over most of the 20th century (Villalba, 1990); however, this relationship weakened since the late 1970s (Lavergne, 2016). This change in the relationship between climate and *F. cupressoides* tree growth has not been attributed to specific standardization techniques applied or to the quality of the climate data used to infer the temperature signal but to specific physiological responses to recent environmental changes. Elsewhere, changes in climate–tree growth relationships have been attributed to the following: (1) an increase of the net primary production due to increasing availability of carbon ($CO_2$ fertilization effect; Ainsworth & Long, 2005; Huang et al., 2007; Norby et al., 1999; Prentice & Harrison, 2009; Wang, 2007); (2) changes in limiting factors of tree growth such as an increasing dependence on nutrient availability (Norby et al., 2010; Peñuelas et al., 2011); or (3) intensification of hydroclimatic variability impacts on growth (Girardin, Hogg, et al., 2016). The concurrent effects of increasing atmospheric $CO_2$ concentrations ($c_a$) and higher temperatures on tree growth are difficult to disentangle. They are expected to further stimulate forest productivity in temperature-limited systems in the absence of drought stress (e.g., Bonan, 2008; Büntgen et al., 2014; Huang et al., 2007; Salzer et al., 2009) or to induce growth decline in water-limited systems if the negative effect of low precipitation is not compensated by the fertilization effect (Allen et al., 2010; Girardin, Bouriaud, et al., 2016; Lévesque et al., 2014; Linares & Camarero, 2011, 2012; Silva et al., 2010; Silva & Madhur, 2013). In contrast with the nonstationary relationships between summer temperatures and *F. cupressoides* growth, Lavergne et al. (2017) showed a stable relationship between $\delta^{13}C$ values and summer temperature over the last 60 years.

Here we test the possibility of combining tree ring width (expressed as basal area increment (BAI)) and $\delta^{13}C$ series from *F. cupressoides* in the eastern slope of the northern Patagonian Andes for reconstructing summer temperature over the past two centuries. We show that the recent enhancement of tree growth recorded is likely attributable to a $CO_2$ fertilization. After correcting for this effect, we test different regression models to

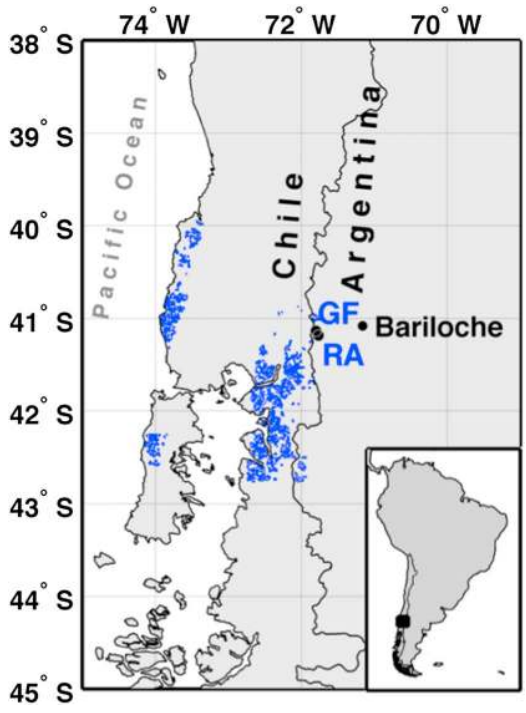


**Figure 1.** Location of the two tree ring sites (Río Frías, GF, and Río Alerce, RA) and Bariloche meteorological station, northern Patagonia, Argentina. The blue area represents the geographical distribution of *Fitzroya cupressoides* computed on ArcGIS based on observations.

reconstruct past temperature variability in southern South America and compare the selected 212 year summer temperature records to previous reconstructions in the region.

## 2. Material and Methods

### 2.1. Tree-Ring Data

Tree cores from *Fitzroya cupressoides* at Glaciar Frías (GF) and Río Alerce (RA) were initially collected during the austral summers in the late 1980s to early 1990s and more recently in 2013. The two sites, at a distance of ~6 km from each other, are located in the Argentinean humid forests of northern Patagonia, between 950 and 1,050 m in elevation (41°09′S, 71°53′W; Figure 1). At each site, paired increment cores at breast height (1.3 m above the ground) were extracted using a Pressler borer (5 mm diameter) from more than 30 trees showing similar competition and microsite conditions. Cores were dated to the calendar year of tree ring formation and cross-dated following Stokes and Smiley (1968). Quality control of ring width measurements and cross dating were conducted with the program COFECHA (Holmes, 1983). Since both sites show similar variations in tree growth (Lavergne, 2016), we merged the samples in a single record. The updated tree ring width (TRW) series from the two sites include 374 cores. They were also detrended and indexed using a negative exponential curve (NEGEX) implemented in the CRUST routine (Melvin & Briffa, 2014) to preserve high- to medium-frequency common growth signal. The standardized series were averaged to produce a single tree ring index (TRI) chronology.

For the period 1952–2011, six trees at each site were selected, and their dated growth rings were annually pooled prior to being analyzed for $\delta^{13}C$. These data were previously published by Lavergne et al. (2017). Consistently with the tree ring width records, similarities in the carbon isotopic chronologies indicate that GF and RA trees can be considered as a single isotopic population (Lavergne et al., 2017). Therefore, for the period 1952–2011, we used the mean value of the two $\delta^{13}C$ site chronologies already published (the data are available at the International Tree-Ring Data Bank (ITRDB) of the NOAA National Climate Date Center; https://www1.ncdc.noaa.gov/pub/data/paleo/treering/isotope/southamerica/argentina/). For the period 1800–1951, we selected the same *F. cupressoides* trees. They were old enough not to introduce any juvenile effects on $\delta^{13}C$. Annual tree rings were split using a scalpel. The wood samples were then chipped and grounded in a ball mill for homogenization. α-Cellulose was extracted from the wood according to the Soxhlet chemical method derived from Leavitt and Danzer (1993). α-Cellulose was homogenized ultrasonically with a sonotrode apparatus and freeze-dried. Cellulose samples of around 0.10 mg were loaded in tin foil capsules. The $\delta^{13}C$ was determined with an elemental analyzer (EA NC2500, Carlo Erba) coupled with a Finnigan MAT252 mass spectrometer. An internal laboratory reference of cellulose (Whatmann® CC31) was used to correct for instrument drift and to normalize the data to internationally accepted standards. Along the sequence analyses, the isotopic composition of CC31 was measured every three samples. The standard deviation (SD) obtained from the measurement of the isotopic composition of 10 consecutive CC31 standards was typically ±0.1‰. The analyses on each sample were repeated at least once and up to three times.

To assess the intertree isotopic variability, we compared annual $\delta^{13}C$ variations from 12 individuals (six at each site) over the period 1920–1951 (Figure S1 in the supporting information). The $\delta^{13}C$ variations from these individuals were well correlated (mean pairwise correlation $r = 0.35$, $p < 0.05$, and standard deviation SD = 0.32). Reflecting this coherence between the isotopic records, the 12 cores provided an expressed population signal (Briffa, 1984; Wigley et al., 1984) of 0.9 and a confidence interval around the mean of 0.4‰. For the period 1800–1920, the 12 trees were pooled prior to analysis to produce a $\delta^{13}C$ chronology representative of the whole population.

### 2.2. BAI and iWUE Calculations

Due to the persistent trend of decreasing ring width with increasing tree diameter and age, patterns of tree growth related to forest growth are better captured using BAI (Rodríguez-Catón et al., 2016). Here BAIs were estimated for each individual tree (a total of 374 trees) from the bark to the pith using the BAI.out( ) function of the R package "dplR" (Figure S2). We considered only the 1800–2011 portion of the mean BAI series.

We then calculated the intrinsic water-use efficiency (iWUE), that is, the ratio of net photosynthesis $A$ to conductance for water vapor $g$, which is defined as follows (Farquhar & Richards, 1984):

$$\mathrm{iWUE} = A/g = (c_a - c_i)\times 0.625 \quad (1)$$

where $c_a$ and $c_i$ are atmospheric and intercellular $CO_2$ concentrations, respectively, calculated from the isotopic discrimination $\Delta^{13}C$ according to the following (Farquhar et al., 1982):

$$c_i = \left(\Delta^{13}C - a\right)/(b - a)\times c_a$$

where $a$ is the diffusion fractionation across the boundary layer and the stomata (≈4.4‰) and $b$ is the RuBisCo enzymatic biological fractionation (≈27‰).

The discrimination, which results from the preferential use of $^{12}C$ over $^{13}C$ during photosynthesis, is related to $\delta^{13}C$ as follows (Farquhar et al., 1982):

$$\Delta^{13}C = \left(\delta^{13}C_{atm} - \delta^{13}C_{raw}\right)/\left(1 + \delta^{13}C_{raw}/1,000\right) \quad (2)$$

Records of $\delta^{13}C_{atm}$ and $c_a$ over the 1850–1999 period were obtained from direct ice core measurements tabulated in McCarroll and Loader (2004), while those for the period 2000–2011 were extracted from records at the South Pole station (Scripps data; Keeling et al., 2005). When both records were available (from 1978 to 2005), we used the means of $\delta^{13}C_{atm}$ and $c_a$ for conducting the corrections.

### 2.3. Assessment of Trends, Physiological Responses, and Relationships With Temperature

We performed the Pettitt's (Pettitt, 1979) and Mann–Kendall's tests (using the pettitt.test( ) and mk.test( ) functions of the R package "trend," respectively) to detect shifts in the long-term trends of iWUE, TRW, TRI, and BAI series over the past 212 years (from 1800 to 2011). The corresponding regression slopes were used as the rates of change through time. To remove potential long-term trends in BAI, we detrended BAI series using a spline of 50% (function loess( ) of R platform) to obtain the BAI residuals (hereafter $BAI_{res}$). We also detected potential shifts from the $BAI_{res}$ series, and assessed the trends and corresponding slopes.

In order to remove the nonclimatic signal from the raw series, the annual $\delta^{13}C_{raw}$ values were corrected for the Suess effect (Keeling, 1979) by removing the preindustrial isotope signature (e.g., −6.4‰, A.D. 1850) from the actual atmospheric $\delta^{13}C_{atm}$ (see Figure S3), such as

$$\delta^{13}C_{cor} = \delta^{13}C_{raw} - \left(\delta^{13}C_{atm} + 6.4\right) \quad (3)$$

Lavergne et al. (2017) demonstrated that the interannual variations of $\delta^{13}C_{cor}$ in *F. cupressoides* are strongly modulated by the temperature of the current growing season (December to February, $T_{DJF}$) in northern Patagonia. Earlier studies have shown that *F. cupressoides* TRWs are more strongly related to previous than current summer temperatures (December to March; Villalba, 1990). We thus chose $T_{DJF}$ as a target and investigated its relationships with tree ring parameters.

We used monthly temperature records from Bariloche, the instrumental weather station on the eastern slopes of the Andes with the longest record (1931–2012) nearest to our sampling sites (41.09°S–71.10°W, 840 m asl; Servicio Meteorológico Nacional; Figure 1). The temperature data were previously homogenized following the procedure described in Lavergne et al. (2015, 2016). We tested the possibility of using both tree ring parameters to develop a multiparametric regression model for reconstructing past $T_{DJF}$ variability. The selection of the regression models showing the maximum likelihood was based on the Akaike information criterion (AIC; Akaike, 1973) and Schwarz's Bayesian Information criterion (BIC) tests. Both tests evaluate the quality of fit of the statistical models. Models with the lowest AIC and BIC show the best skills. We then conducted the calibration–verification tests using half of the summer temperature series for calibration and half for assessing the reconstruction quality (verification). To assess the predictive skill of the models, the coefficient of determination ($r^2$) of the regression models, reduction of error statistic (RE; Fritts, 1976),

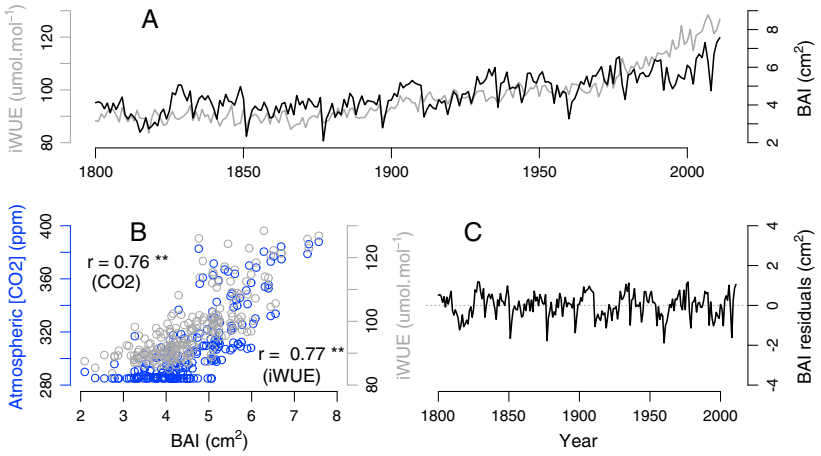


**Figure 2.** (a) Variations in intrinsic water-use efficiency (iWUE, gray) and basal area increment (BAI, black) over the 1800–2011 period. (b) Correlations between iWUE and atmospheric $CO_2$ (ppm) and BAI ($cm^2$) over the same period. (c) Temporal variations of BAI residuals estimated using three different corrections (extracting iWUE or $c_a$ trends from BAI series, or using a 50% spline; gray, blue and black, respectively). The ** indicates that the correlation is significant at 99% confidence level.

coefficient of efficiency (CE; Cook et al., 1994), and Durbin–Watson statistic (DW; Durbin & Watson, 1971) were systematically compared for independent calibration and verification periods. The coefficient of determination ($r^2$) indicates the extent to which two series covary but is insensitive to any offset in the absolute values. The RE and CE are measures of shared variance between target and proxy series. They compare the fit between measured and reconstructed values (root mean squared error (RMSE)) with the fit obtained by simply using the calibration mean (RE) or verification mean (CE) of the actual data. Positive values for these two tests indicate predictive skill of the regression models. The DW tests for first-order autocorrelation in the model residuals. A DW value of around 2 indicates no first-order autocorrelation in the residuals (Durbin & Watson, 1971). Regressions, AIC–BIC, and statistical tests were performed using the R software environment (lm( ) and predict( ) functions, the R package "MuMin," and skills( ) function of the R package "treeclim"; Zang & Biondi, 2015). The best models providing the more reliable estimation of summer temperature variability over the period 1931–2011 were applied in reconstructing temperature variations over the period 1800–2011.

### 2.4. Spectral Properties of the Summer Temperature Reconstructions

We investigated the relation of the $T_{DJF}$ reconstructions with large-scale climate forcings from low (El Niño–Southern Oscillation (ENSO)) and high latitudes (Southern Annular Mode (SAM)) using the following indicators of ENSO (1 and 2) and SAM (3 and 4): (1) reconstructed sea surface temperatures (SST) as represented by the Niño 3.4 index from Li et al. (2013) over the 1800–2005 period; (2) December–February Niño 3.4 Index data set extracted from the NCAR Climate Analysis Section Data Catalog (http://www.cgd.ucar.edu/cas/catalog/climind/TNI_N34/index.html) covering the period 1870–2011; (3) reconstructed SAM (Villalba et al., 2012) indices over the common period 1800–2006; and (4) December–February SAM index from

**Table 1**
*Temporal Trends in iWUE ($\mu mol\ mol^{-1}\ yr^{-1}$), TRW ($\mu m\ yr^{-1}$), TRI (Unit $yr^{-1}$), and BAI ($cm^2\ yr^{-1}$) Evaluated Using Mann–Kendall Trend Test*

| Period | iWUE | Period | TRW | Period | TRI | Period | BAI |
|---|---|---|---|---|---|---|---|
| 1800–1903 | *ns* | 1800–1927 | −0.37* | 1800–1927 | *ns* | 1800–1923 | 0.005** |
| 1904–1971 | 0.07** | 1928–2011 | *ns* | 1928–2011 | 0.008* | 1924–1966 | *ns* |
| 1972–2011 | 0.61** | | | | | 1967–2011 | 0.03** |
| 1800–2011 | 0.12** | 1800–2011 | *ns* | 1800–2011 | 0.008** | 1800–2011 | 0.01** |

*Significant at 95% confidence level. **Significant at 99% confidence level.
*ns*: nonsignificant.

**Table 2**
*Lag-1 Autocorrelation (Autocor) of Each Series and Correlation With Mean Temperature for Previous ($T_{pDJF}$) and Current Summer ($T_{DJF}$) Over the 1931–2011 Period*

| Parameter | Autocor | $T_{pDJF}$ | $T_{DJF}$ |
|---|---|---|---|
| TRW | 0.52** | −0.27** | *ns* |
| TRI | 0.34** | −0.28* | *ns* |
| BAI | 0.50** | *ns* | *ns* |
| $BAI_{res}$ | 0.33** | −0.36** | *ns* |
| $\delta^{13}C_{cor}$ | *Ns* | *Ns* | 0.79** |

*Significant at 95% confidence level. **Significance at 99% confidence level. *ns*: nonsignificant.

Marshall (2003) over the 1957–2011 period (extracted from the British Antarctic Survey platform; http://www.nerc-bas.ac.uk/icd/gjma/sam.html). We also conducted time–space cross-wavelet analyses to identify the spectral properties of the reconstructions and their links to ENSO and SAM using the xwt( ) function of the R package "biwavelet."

## 3. Results

### 3.1. Trends in iWUE and Tree Growth Series

Globally, the intrinsic water-use efficiency increases by 0.12 μmol $mol^{-1}$ $yr^{-1}$ over the period 1800–2011 (Figure 2a, Table 1). Based on the Pettitt's test, three main periods in iWUE annual variations are recognized. From 1800 to 1903, the iWUE fluctuates around ~90 μmol $mol^{-1}$ with no significant trend. From 1904 to 1971, the iWUE increases from ~90 to 100 μmol $mol^{-1}$ at a mean rate of ~0.07 μmol $mol^{-1}$ $yr^{-1}$. Finally, a large increase from ~100 to 125 μmol $mol^{-1}$ is recorded between 1972 and 2011 at a mean rate of ~0.61 μmol $mol^{-1}$ $yr^{-1}$. The TRW and TRI variations can also be divided in two parts: from 1800 to 1927, the TRW decreases by ~0.37 μm $yr^{-1}$, while the TRI stays constant. In comparison between 1928 and 2011, TRW stays constant, and TRI increases at a rate of ~0.008 unit $yr^{-1}$ (Table 1). Finally, BAI increases from ~4 to ~5 $cm^2$ at a rate of ~0.005 $cm^2$ $yr^{-1}$ over the period 1800–1923, remains constant at around ~5 $cm^2$ from 1924 to 1966, and finally increases from ~5 to almost 7 $cm^2$ at a rate 0.03 $cm^2$ $yr^{-1}$ between 1967 and 2011 (Figure 2a, Table 1).

Variations in BAI and in iWUE are strongly related to changes in atmospheric $CO_2$ concentration ($c_a$; $r \approx 0.77$, $p < 0.01$; Figure 2b). These relationships mostly rely on their common low-frequency variations. A comparison of the high-frequency oscillations of these series suggests that $c_a$ is not significantly related to BAI ($p = 0.9$), while iWUE shows a weak but significant relationship with BAI ($r = 0.15$, $p < 0.05$). The $BAI_{res}$ series, resulting from the detrending of BAI, does not show significant trend (Figure 2c).

### 3.2. Relationships With Summer Temperature

Over the 1931–2011 period, the raw TRW and TRI chronologies are moderately but significantly related to previous growing season $T_{pDJF}$ ($r \approx -0.27$, $p < 0.01$; Table 2), while the BAI chronology is not. The $T_{pDJF}$ signal is more strongly recorded in $BAI_{res}$ than in both TRW and TRI series ($r = -0.36$, $p < 0.01$). No significant relationships are registered using temperatures of the current growing season. In accordance with results from Lavergne et al. (2017), the $\delta^{13}C_{cor}$ chronology is not significantly related to previous summer temperatures but strongly related to current summer temperatures ($r = 0.79$, $p < 0.01$; Table 2).

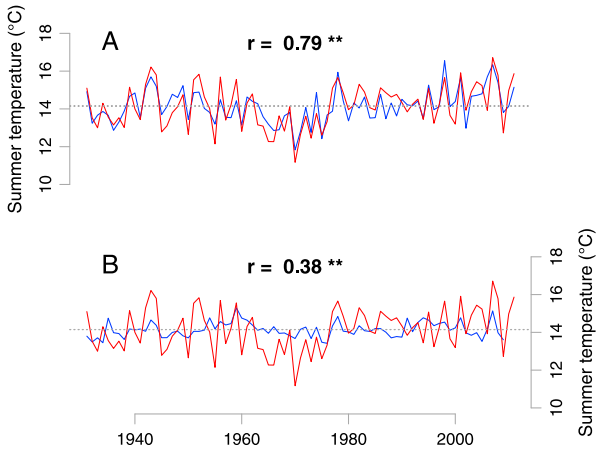


**Figure 3.** Comparison between reconstructed (blue) and observed (red) summer temperature from Bariloche station over the calibration period 1931–2011 for the (A) $\delta^{13}C_{cor}$-based and (B) $BAI_{res}$-based regression models. The standard deviation of the summer temperature series is 1.12 for the observation and 0.89 (0.39) for the reconstruction based on $\delta^{13}C_{cor}$ ($BAI_{res}$) over the 1931–2011 period. The ** indicates that the correlation is significant at 99% confidence level.

### 3.3. Tree Ring Based Summer Temperature Reconstructions

Given that $\delta^{13}C_{cor}$ and $BAI_{res}$ are significantly correlated to summer temperatures, they could theoretically be combined to develop a multiparameter regression model. However, they are also significantly intercorrelated over the 1800–2011 period ($r = -0.21$, $p < 0.01$) and particularly over the calibration period 1931–2011 ($r = -0.37$, $p < 0.01$), suggesting that the temperature signal recorded in tree ring growth is not substantially different from the $\delta^{13}C$ signal. Moreover, the Akaike tests rejected this multiregression model. We therefore chose to adopt two regression models, one based on $\delta^{13}C_{cor}$ and the other one on $BAI_{res}$, to produce two distinct 212 year long summer temperature reconstructions (Figures 3 and 4; Table 3).

Split-period verifications of the calibrated relationships (Table 3) confirm that the linear regression model based on $\delta^{13}C_{cor}$ (over 1931–2011) is reliable and has high predictive skills ($r_{adj}^2 = 0.62$, RE > 0, CE > 0, and RMSE < 0.7°C). A DW statistic of around 1.83 for

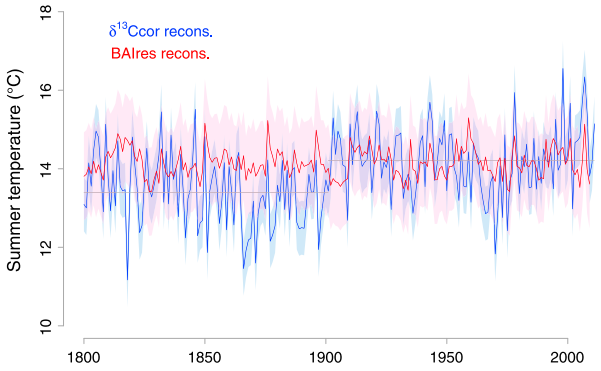


**Figure 4.** Summer temperature reconstruction variations based on $\delta^{13}C_{cor}$ (blue) and averaged $BAI_{res}$ (red) over the period 1800–2011. The shaded blue (red) represents the confidence intervals (±RMSE = 0.69°C or 1.15°C, respectively). The changes in mean temperature levels detected with the Pettitt's test for the reconstruction based on $\delta^{13}C_{cor}$ are shown in gray (mean of 13.4°C before 1903 and 14.2°C after 1903).

this model, whatever the calibration period considered, suggests only minimal residual autocorrelation. As expected, the predictive skills for the calibration model based on $BAI_{res}$ in year $t + 1$ are comparatively lower ($r_{adj}^2 = 0.11$; DW = 1.45, RMSE = 1.15°C, RE > 0 but CE < 0).

According to the $\delta^{13}C_{cor}$-based temperature reconstruction, the coldest summer interval of the last two centuries spans from 1850 to 1900. In the 20th century, a relative cold period occurred in the early 1970s (Figure 4). The mean summer temperatures increased +0.6°C from the 19th to the 20th century (shift in year 1903 following the Pettitt's test). In contrast, over the 1800–2011 period, the $BAI_{res}$-based reconstruction exhibits neither important variations nor any shift in mean temperatures. The standard deviation of the latter reconstruction is half that based on isotopes over the whole period (SD = 0.42 versus 0.95, respectively). The reconstructions are significantly, although weakly, correlated to one another over 1800–2011 ($r = 0.21$, $p < 0.01$). Fifty-one-year sliding correlations between them reveal that they are more similar in the last decades (i.e., $r = 0.37$, $p < 0.01$, over the period of calibration 1931–2011; Figure S4).

### 3.4. Impacts of Large-Scale Forcings on Summer Temperatures

The two $\delta^{13}C_{cor}$- and $BAI_{res}$-based $T_{DJF}$ reconstructions are significantly correlated to the December–February SAM-Marshall index over the period 1957–2010 ($r = 0.37$, $p < 0.01$, and $r = 0.27$, $p < 0.05$, respectively) but not significantly to the Niño 3.4 index. The relationships between the two reconstructions and the climate forcings seem to be nonstationary. The $\delta^{13}C_{cor}$-based reconstruction is significantly correlated to the reconstructed SSTs of Li et al. (2013) over the second half of the 19th century and to the reconstructed SAM indices of Villalba et al. (2012) over the second half of the 20th century (Figures S5A and S5B). In comparison, the $BAI_{res}$-based $T_{DJF}$ reconstruction is significantly related to the reconstructed SSTs of Li et al. (2013) over a more extended period from late 19th to mid-20th century as well as to the reconstructed SAM indices of Villalba et al. (2012) from mid-19th to mid-20th century (Figures S5C and S5D).

The time–space cross-wavelet analysis shows that our $\delta^{13}C_{cor}$-based reconstruction is associated with ENSO at periods of 8 to 12 years over the 1870–1925 period, whereas intermittent common oscillations shorter than 8 years are observed after 1925 (Figure 5a). Similar observations are detected using the Niño 3.4 index data set (Figure 5b). Moreover, this temperature reconstruction is associated with the reconstructed SAM indices of Villalba et al. (2012) at periods shorter than 8 years over the 1800–1870 period and shorter than 6 years since 1870 (Figure 5c). Notably, in the late 20th to early 21st century, a strong common period of variability shorter than 4 years is observed between the two series, which is more pronounced using the SAM data of Marshall (2003) over the 1957–2011 period (Figure 5d). Finally, in the early to mid-1970s, both $\delta^{13}C_{cor}$-based $T_{DJF}$ reconstruction and SAM-Marshall series show common oscillations of less than 3 years. Similar oscillations of common variability, but of lower intensity, are detected between the $BAI_{res}$-based $T_{DJF}$ reconstruction and the tropical and high-latitude forcings (Figure S6).

**Table 3**
*Calibration and Verification Statistics of the Tree Ring Chronologies Against Summer (December–February) Temperature Using Simple Regressions*

| | Calibration | | | | Verification | | | | |
|---|---|---|---|---|---|---|---|---|---|
| Model | Period | $r_{adj}^2$ | RMSE | DW | Period | RMSE | $r_{adj}^2$ | RE | CE |
| $\delta^{13}C_{cor}$ | 1931–1970 | 0.69** | 0.64 | 1.855 | 1971–2011 | 0.78 | 0.54** | 0.487 | 0.368 |
| | 1971–2011 | 0.54** | 0.76 | 1.803 | 1931–1970 | 0.67 | 0.69** | 0.611 | 0.577 |
| $BAI_{res}$ ($t + 1$) | 1931–1970 | 0.10* | 1.24 | 1.629 | 1971–2011 | 1.12 | 0.12* | 0.124 | −0.079 |
| | 1971–2011 | 0.12* | 1.01 | 1.246 | 1931–1970 | 1.31 | 0.10* | 0.080 | −0.001 |

*Note.* $r_{adj}^2$: coefficient of determination adjusted for loss of degrees of freedom; RMSE: root mean squared error of the estimate for two independent periods; DW: Durbin–Watson statistic; RE: reduction of error statistic; CE: coefficient of efficiency.
*Significance at 95% and 99% confidence level. **Significance at 95% and 99% confidence level.
Overall period (1931–2011) for $\delta^{13}C_{cor}$: $r_{adj}^2 = 0.62$, DW = 1.927, RMSE = 0.69; and for $BAI_{res}$: $r_{adj}^2 = 0.11$, DW = 1.45, RMSE = 1.15.

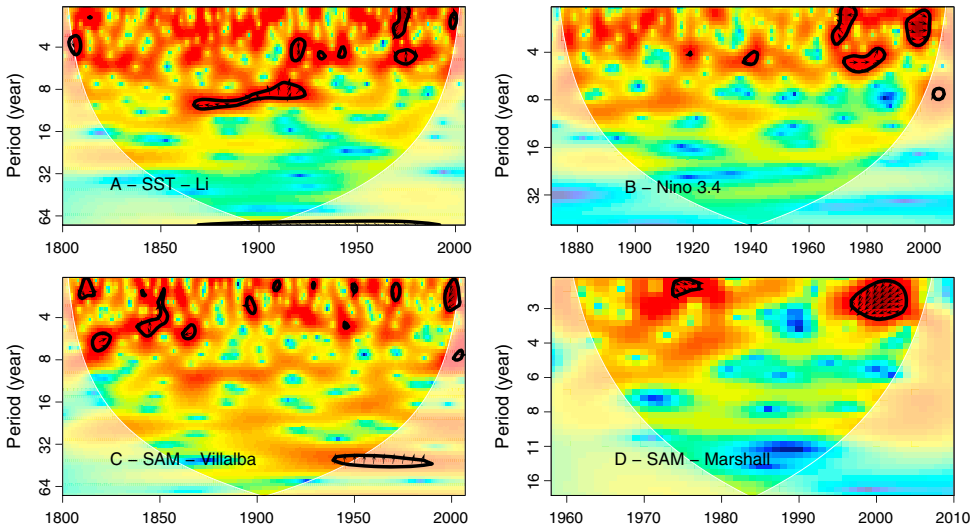


**Figure 5.** Cross-wavelet analysis (XWT) between the summer temperature reconstruction based on $\delta^{13}C_{cor}$ and (a) sea surface temperature, an indicator of ENSO (Li et al., 2013) over the common period 1800–2005, (b) December–February Niño 3.4 time series over the common period 1870–2011 (extracted from https://www.esrl.noaa.gov/psd/enso/data.html), (c) reconstructed SAM (Villalba et al., 2012) indices over the common period 1800–2006, and (d) December–February SAM index from Marshall (2003) over the 1957–2011 period (extracted from http://www.nerc-bas.ac.uk/icd/gjma/sam.html).

## 4. Discussion

### 4.1. Physiological Response of *Fitzroya cupressoides* to Increasing Atmospheric $CO_2$

The BAI and iWUE records of *Fitzroya cupressoides* are significantly related, showing a similar increasing trend particularly after ~1970. As iWUE represents the ratio between carbon assimilated and water transpired (Frank et al., 2015; Voelker et al., 2015), higher iWUE could be due to either greater carbon assimilation in response to increased $c_a$, lower transpiration in response to a reduction in water availability, or a combination of both. Using $\delta^{13}C_{cor}$ and $\delta^{18}O$ data, Lavergne et al. (2017) showed that over the period 1952–2011, the iWUE enhancement in *F. cupressoides* was more likely due to an increase in carbon assimilation rate rather than to a decrease in the stomatal conductance, although the latter may have also changed over time. The increase in BAI also points to an enhancement of the carbon uptake. In consequence, the parallel increases in BAI and iWUE are consistent with a scenario of $CO_2$ fertilization.

The response of *F. cupressoides* to increasing $c_a$ observed here is consistent with the work by Urrutia-Jalabert, Rossi, Deslauriers, et al. (2015) on the western slope of the Andean Cordillera at the rainy Alerce Andino National Park (Chile, 41°32′S–72°35′W). Indeed, they showed that trees on the western slope of the Andes have been more efficient in water use over the last decades, probably by increasing their photosynthetic rates, leading to an increase of tree growth. This has been likely driven by a combination of $CO_2$ and/or surface radiation increases (Urrutia-Jalabert, Rossi, Deslauriers, et al., 2015). However, there are some evidences that *F. cupressoides* trees in contrasting environments respond differently to increasing $c_a$. Although iWUE has increased in *F. cupressoides* since the 1900s at both the Chilean coast (Alerce Costero National Park, Chile, 40°10′S–73°26′W) and the Andean Cordillera, tree growth has decreased since the 1980s in the coastal region due to increasing drying conditions (Urrutia-Jalabert, Rossi, Deslauriers, et al., 2015). The increase in iWUE under drier conditions should be therefore mostly related to a decrease in stomatal conductance. Further south in the temperate rainforests on the western slope of the Andes (Huinay Private Park, Chile, 42°23′S–72°25′W), Camarero and Fajardo (2017) have shown that neither growth nor iWUE have steadily increased over the last decades. Indeed, tree growth and iWUE started to decrease since the 1980s concurrent with drier and warmer conditions during the growing season. The authors pointed to a poor acclimation of this species to hydrological changes even in normally well-drained sites, particularly at young stands (<300 years of age), which were established during the postindustrial $c_a$ period. Therefore, the physiological response of *F. cupressoides* to increasing $c_a$ appears to be significantly modulated by site-specific conditions, recent changes in precipitation, and tree ages. It is worth noting that *F. cupressoides* has one of the longest

carbon residence time ever observed in the word (Urrutia-Jalabert, Malhi, Barichivich, et al., 2015). Sensitivity analysis of tree growth to increasing $c_a$ using process-based vegetation models would allow testing the hypothesis of $CO_2$ fertilization effect (Girardin et al., 2011) and better assess the main physiological processes influencing *F. cupressoides* growth in recent decades. Carbon, water, and energy budgets derived from eddy covariance measurements will help to understand how variations in iWUE at the ecosystem level are translated into productivity changes (Babst et al., 2014; Belmecheri et al., 2014), which in turn will improve our description of *F. cupressoides* carbon sink patterns under changing environmental constraints.

### 4.2. Climate Influence on Tree Ring Records

Interannual variations in radial growth of *F. cupressoides* ($BAI_{res}$) are negatively related to summer temperature during the previous growing seasons. These findings imply that warm summers have a net negative impact on interannual growth. On the other hand, warm conditions can increase the length of the growing season and therefore the opportunities to fix carbon (Wolkovich et al., 2012). Therefore, we would expect growth and temperature to be positively correlated. However, increased annual radial growth can be achieved only if other requirements for growth are also met. Indeed, other warming-induced processes can affect tree growth and attenuate or counteract this response, that is, the water limitation on photosynthesis resulting from higher evapotranspiration and the higher metabolic cost of plant maintenance induced by higher temperatures (Girardin, Bouriaud, et al., 2016; McDowell et al., 2011). Urrutia-Jalabert et al. (2015) demonstrated that the negative relationship between radial growth (ring width and BAI) and temperature in *F. cupressoides* in the Chilean Andes was mediated through the effect of temperature on vapor pressure deficit. The negative relationship with previous year summer temperature may also result from a reduced assimilation of carbon in response to stomata closure under warmer and drier conditions, as it has been recently proposed by Camarero and Fajardo (2017; see previous section). If less carbon is assimilated during a dry growing season, less is likely to be allocated to storage compartments and used for early wood synthesis at the beginning of the following growing season, leading consequently to a narrower ring (Deslauriers et al., 2014; Urrutia-Jalabert et al., 2015). Therefore, although the increase in atmospheric $CO_2$ levels could have boosted the photosynthesis of *F. cupressoides* at our sites causing a long-term increase in tree ring growth, the interannual variability of radial growth has also been affected by year-to-year changes in water availability.

In contrast to radial growth, the temperature signal during the current growing season is positively and strongly recorded in the $\delta^{13}C_{cor}$ series. Over the same comparison period (1931–2011), more than half of the interannual variance in $\delta^{13}C_{cor}$ is explained by summer temperature variations ($r^2_{adj} = 0.62$, $p < 0.001$, adjusted for loss of degrees of freedom). As discussed in Lavergne et al. (2017), this strong $\delta^{13}C_{cor}$–summer temperature relationship reflects the imprint of solar radiation on carbon isotopic fractionation. Indeed, when photosynthesis decreases in response to light limitation, the leaf internal $CO_2$ concentration ($c_i$) increases, which in turn increases the carbon discrimination against $^{12}C$ ($\Delta^{13}C$ proportional to $c_i/c_a$ ratio) leading to a decrease of $\delta^{13}C$ (Farquhar et al., 1989). This hypothesis is in agreement with the decreasing trend in cloud fraction (−4%) and increasing trend in photosynthetically active radiations (+3.5%) observed in the region over the 1984–2007 period (data retrieved from NASA/GEWEX Surface Radiation Budget; see Lavergne et al., 2015). Thus, in line with the literature, environmental conditions favorable to forest productivity (here, cool summers with less sunlight) result in higher $\Delta^{13}C$ during carbon assimilation and therefore lower $\delta^{13}C$, than do conditions unfavorable to growth (Raczka et al., 2016).

### 4.3. A 212 Year Summer Temperature Reconstruction for Northern Patagonia

The $\delta^{13}C_{cor}$ and $BAI_{res}$ records were used as single predictors to reconstruct past variations in summer temperature on the eastern slopes of the northern Patagonian Andes. Clearly, the regression model based on $\delta^{13}C_{cor}$ displays the strongest predictive skills. Interestingly, the two $T_{DJF}$ reconstructions are becoming more similar over the last decades. Given that variations in $\delta^{13}C_{cor}$ are the most strongly related to summer temperatures, the recent similarity between the reconstructions suggests that tree growth variability is likely more sensitive to temperature variations in the warmer context of the last decades than before.

The $\delta^{13}C_{cor}$-based reconstruction reveals that the 20th and early 21st centuries have been warmer (+ 0.6°C) than the 19th century. Warmer conditions over the 20th century were interrupted by a colder period in the early 1970s. After that, summer temperature has increased up to its present level. The multidecennial

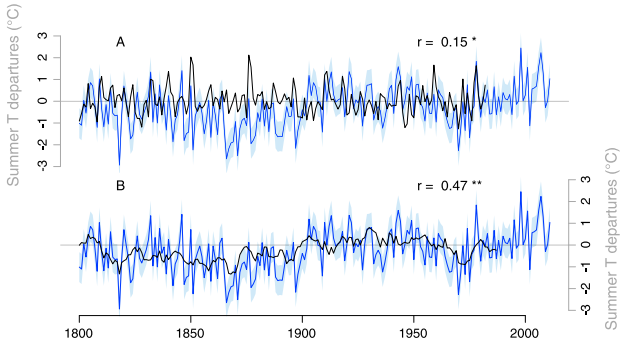


**Figure 6.** Comparison of the $\delta^{13}C_{cor}$-based (blue) reconstruction with (a) the Villalba (1990) summer reconstruction based on the treering width chronology of *Fitzroya cupressoides* at 41°S for the overlapping period 1800–1984 ($r = 0.15$, $p < 0.05$) and (2) the Villalba et al. (2003) reconstruction for the Northern Patagonian Andes based on the first principal component of tree ring width records from *Nothofagus pumilio* for the overlapping period 1800–1987 ($r = 0.47$, $p < 0.01$). The summer temperature anomalies are calculated using the 1901–1995 climatology. The shaded blue represents the confidence intervals for each reconstruction (±1 RMSE= 0.69°C). The * and ** indicate that the correlation is significant at 95% and 99% confidence level, respectively.

variations in summer temperature over the last two centuries reconstructed here are significantly, but weakly, related to previous reconstructions based on *Fitzroya cupressoides* ring width records from the same stands (Villalba, 1990; $r = 0.15$, $p < 0.05$, 1800–1984; Figure 6a). The most notable difference between the two reconstructions lies in the reduction of the multidecadal temperature variability in the ring width based reconstruction (Villalba, 1990). Indeed, in the early study by Villalba (1990), flexible standardization methods were applied to the tree ring records, maximizing the interannual variations of the reconstruction at the expense of the longer term variations. Therefore, the low consistency between the two reconstructions is likely due to the different spectral domains of temperature variability reconstructed. Notably, our reconstruction explains ~25% more variance in summer temperature than the previous work by Villalba (1990) over the same calibration period ($r^2_{adj} = 0.68$ versus $r^2_{adj} = 0.42$ over 1931–1984). As expected, our second reconstruction based on $BAI_{res}$ records, which is derived from an updated version of the ring width chronology previously developed by Villalba (1990), is highly and significantly related to this reconstruction ($r = 0.77$, $p < 0.01$, Figure S7A) and is capturing as much high-frequency variance as that in the earlier reconstruction (Villalba, 1990).

The $\delta^{13}C_{cor}$-based reconstruction also agrees well with a mean temperature reconstruction for northern Patagonia based on tree ring width records from *Nothofagus pumilio*, the dominant subalpine tree across the southern Andes (Villalba et al., 2003; Figure 6b). It is important to mention here that unlike our temperature reconstructions for the eastern slope of the Andes, Villalba et al. (2003) reconstructed the mean annual temperature variations resulting from averaging three records in the Chilean slope of the Andes (Puerto Montt, Valdivia, and Temuco). Since the reconstruction of Villalba et al. (2003) is not a seasonal but an annual reconstruction intended to retain as much low-frequency variance as possible, its interannual variability is by construction lower than ours in the common 1800–1987 period (SD = 0.46 versus SD = 0.91, respectively). Both reconstructions share, however, some common variability ($r = 0.47$, $p < 0.01$). The percentage of variance explained in our temperature reconstruction is higher than that in Villalba et al. (2003; $r^2_{adj} = 0.66$ versus $r^2_{adj} = 0.55$ over 1931–1987). In contrast, our second reconstruction based on $BAI_{res}$ series is not significantly related to that of Villalba et al. (2003). Both records have similar variance around the mean (SD ≈ 0.45), however, they largely differ in terms of long-term variability with opposite variations in decadal temperature oscillations mostly over the 19th century (Figure S7B). This opposite pattern in multidecadal temperature trends has also been recorded in instrumental records located on both sides of the Andes (see section 4.4; Villalba et al., 2003). Compared to these two already published reconstructions and to the one based on $BAI_{res}$, the advantage of our $\delta^{13}C_{cor}$-based reconstruction is that the low- and high-frequency variations in temperature are equally retained. Its strength is then doubled: it can be used to study multidecadal variations in temperature as well as extreme warm or cold events. For instance, 38% of the extreme values in the observations are also detected in the prediction (with ±1.5 × SD as a threshold; not shown).

### 4.4. Summer Temperature Variability Related to Low-Latitude (ENSO) and High-Latitude (SAM) Climate Forcings

At approximately 41°S over the Andes, temperature variations are not only influenced by the Southern Annular Mode, the leading mode of climate variability at higher latitudes in the Southern Hemisphere, but also by the El Niño–Southern Oscillation rooted at lower latitudes in the Pacific Ocean (Garreaud et al., 2013). As mentioned above, temperature variations are nonuniform over the Andes and the adjacent regions. While summer temperatures from Bariloche station on the east side of the northern Patagonian Andes (41°12′S–71°12′W, 840 m asl) have increased at ~0.2°C per decade since the 1950s (Lavergne et al., 2017; Villalba et al., 2003), a significant decrease of ~0.2°C per decade in summer has been recorded from 1950s onward at Puerto Montt, located on the western side of the Andes near the Pacific coast (41°25′S, 73°05′W, 14 m asl) (Camarero & Fajardo, 2017; Villalba et al., 2003). Moreover, while instrumental records from

Valdivia coastal station (39°48′S, 73°14′W, 9 m asl) have depicted a significant warming trend over the period 1960–2010 (Urrutia-Jalabert, Rossi, Deslauriers, et al., 2015), no clearly identifiable trends were reported in southern Chile (38°S–48°S) for the period 1979–2006 (Falvey & Garreaud, 2009). Interestingly, significant surface cooling at coastal stations (0.2°C/decade) and warming in the Andes (+0.25°C/decade) were detected further north in central and northern Chile (17°S–37°S) for the period 1979–2006 (Falvey & Garreaud, 2009). These different patterns emphasize the strong spatial variability of temperature in the region. Nevertheless, a short common cold period from 1950 to 1975 was observed at both Andean slopes (Villalba et al., 2003). This cold period was followed by a regional jump in temperature around 1976, associated with a well-documented increase in SST in the tropical Pacific (Mantua et al., 1997; Trenberth & Hurrell, 1994). Based on these observations, it is worth noting that our summer temperature reconstruction are mainly representative of climate variations on the eastern slopes of the Andes in northern Patagonia, which are largely modulated by interannual and decadal oscillations rooted in both high and low latitudes.

Correlation and spectral analyses also demonstrate that the temperature signals imprinted in *F. cupressoides* growth and $\delta^{13}C_{cor}$ have been modulated by oscillatory modes at interannual to secular scales related to ENSO and SAM. Interestingly, the strong commonality in decadal oscillations between the tropical SSTs reconstructed by Li et al. (2013) and our temperature reconstruction from the mid-19th to the early 20th century is concomitant with the highest rate of temperature increase recorded over the last 360 years in northern Patagonia (Villalba et al., 2003). Notably, extreme warm summers related to severe El Niño events such as those in 1877 and 1897 (Markgraf & Diaz, 2000) are more prominent in the ring width based than in the $\delta^{13}C_{cor}$-based reconstruction. The marked common interannual to decadal variability with SSTs indices in the 1970s is likely the imprint of the step increase in SSTs also reported in the temperature records in both sides of the Andes (see above). Such abrupt increase has been related to the shift from negative (cold) to positive (warm) phase of the ENSO-like multidecadal climate variability, often referred to as the Pacific Decadal Oscillation (Mantua & Hare, 2002). A similar marked common interannual variability is also observed with SAM indices in the 1970s and later in the 1990s. Thus, large-scale climatic forcings have a strong impact on local temperature variability, and their climate imprints are strongly recorded in our $T_{DJF}$ reconstructions for the eastern slope of the Andes in northern Patagonia.

## 5. Conclusions

In this study, we developed robust 212 year long BAI and $\delta^{13}C$ chronologies from living *Fitzroya cupressoides* in Northern Patagonia, Argentina (41°S). After correcting the basal area increments to remove the increasing trend likely linked to increasing $CO_2$ concentrations, we tested the possibility of reconstructing past summer temperature variations using different regression models. The combination of the two predictors does not significantly improve the predictive skills of the final regression model. Comparatively, the isotope-based reconstruction has the strongest predictive skills explaining 62% of the total variance in summer temperature over the period 1931–2011. In addition, the low frequency component of our $\delta^{13}C$-based reconstruction agrees well with documented multidecadal variations of summer temperature in north-eastern Patagonia. The summer temperature reconstruction shows two cold periods, in the second half of the 19th century and in the middle of the 20th century followed by a warming trend until the present. Both low-latitude (ENSO) and high-latitude (SAM) climate forcings are modulating climate variations across midlatitudes in South America, with periods dominated by tropical (ENSO) or subantarctic (SAM) influences. Our contribution provides the first reconstruction of summer temperature in South America south of 40°S for the period 1800–2011 entirely based on isotopic records.

**Acknowledgments**
This research was partially supported by LEFE-PATISO project from CNRS-INSU (2012–2014), CONICET Argentina, and the Australian Research Council (ARC DP120104320). A.L. has been supported by a Research associate/Lecturer position at the University of Versailles—St Quentin (UVSQ, France). We acknowledge all data providers: the Argentinian National Meteorological Service, the NCAR Climate Analysis project (http://www.cgd.ucar.edu/cas/catalog/climind/TNI_N34/index.html), the British Antarctic Survey (http://www.nerc-bas.ac.uk/icd/gjma/sam.html), and the NASA/GEWEX Surface Radiation Budget (https://gewex-srb.larc.nasa.gov/). All tree ring data set will be available in the International Tree-Ring Data Bank (ITRDB) of the NOAA National Climate Date Center (https://www1.ncdc.noaa.gov/pub/data/paleo/treering/isotope/southamerica/argentina/). We thank the two anonymous reviewers that have considerably helped improve this manuscript. Finally, we would like to dedicate this work to the independence of the research and the engagement of scientists with policy makers, which are highly valuable in our changing world.

## References

Ahmed, M., Anchukaitis, K. J., Asrat, A., Borgaonkar, H. P., Braida, M., Buckley, B. M., … Zorita, E. (2013). Continental-scale temperature variability during the past two millennia. *Nature Geoscience*, *6*(6), 503–503. https://doi.org/10.1038/ngeo1849

Ainsworth, E. A., & Long, S. P. (2005). What have we learned from 15 years of free air $CO_2$ enrichment (FACE)? A meta-analytic review of the response of photosynthesis, canopy properties and plant production to rising $CO_2$. *New Phytologist*, *165*, 351–372. https://doi.org/10.1111/j.1469-8137.2004.01224.x

Akaike, H. (1973). Information theory and an extension of the maximum likehood principle. In *Second International Symposium on Information Theory* (pp. 267–281). New York: The Econometric Society. https://doi.org/10.2307/2938260

Allen, C. D., Macalady, A. K., Chenchouni, H., Bachelet, D., McDowell, N., Vennetier, M., … Cobb, N. (2010). A global overview of drought and heat-induced tree mortality reveals emerging climate change risks for forests. *Forest Ecology and Management*, *259*, 660–684. https://doi.org/10.1016/j.foreco.2009.09.001

Babst, F., Alexander, M. R., Szejner, P., Bouriaud, O., Klesse, S., Roden, J., … Trouet, V. (2014). A tree-ring perspective on the terrestrial carbon cycle. *Oecologia*. https://doi.org/10.1007/s00442-014-3031-6

Belmecheri, S., Maxwell, R. S., Taylor, A. H., Davis, K. J., Freeman, K. H., & Munger, W. J. (2014). Tree-ring $\delta^{13}C$ tracks flux tower ecosystem productivity estimates in a NE temperate forest. *Environmental Research Letters*, *9*(7), 74011. https://doi.org/10.1088/1748-9326/9/7/074011

Bonan, G. B. (2008). Forests and climate change: forcings, feedbacks, and the climate benefits of forests. *Science*, *320*, 1444–1449. https://doi.org/10.1126/science.1155121

Boninsegna, J. A., Argollo, J., Aravena, J. C., Barichivich, J., Christie, D., Ferrero, M. E., … Villalba, R. (2009). Dendroclimatological reconstructions in South America: A review. *Palaeogeography, Palaeoclimatology, Palaeoecology*, *281*, 210–228.

Briffa, K. R. (1984). *Tree Climate Relationships and Dendroclimatological Reconstructions in the British Isles*. Norwich, UK: Univ. of East Anglia.

Büntgen, U., Frank, D. C., Neuenschwander, T., & Esper, J. (2012). Fading temperature sensitivity of Alpine tree growth at its Mediterranean margin and associated effects on large-scale climate reconstructions. *Climatic Change*, *114*, 651–666. https://doi.org/10.1007/s10584-012-0450-4

Büntgen, U., Tegel, W., Kaplan, J. O., Schaub, M., Hagedorn, F., Bürgi, M., … Liebhold, A. (2014). Placing unprecedented recent fir growth in a European-wide and Holocene-long context. *Frontiers in Ecology and the Environment*, *12*(2), 100–106. https://doi.org/10.1890/130089

Camarero, J. J., & Fajardo, A. (2017). Poor acclimation to current drier climate of the long-lived tree species *Fitzroya cupressoides* in the temperate rainforest of southern Chile. *Agricultural and Forest Meteorology*, *239*, 141–150. https://doi.org/10.1016/j.agrformet.2017.03.003

Cook, E. R., Briffa, K. R., & Jones, P. D. (1994). Spatial regression methods in dendroclimatology: A review and comparison of two techniques. *International Journal of Climatology*, *14*(4), 379–402. https://doi.org/10.1002/joc.3370140404

D'Arrigo, R. D., Wilson, R., Liepert, B., & Cherubini, P. (2008). On the "divergence problem" in northern forests: A review of the tree-ring evidence and possible causes. *Global and Planetary Change*, *60*, 289–305. Retrieved from http://linkinghub.elsevier.com/retrieve/pii/S0921818107000495

Daux, V., Edouard, J. L. L., Masson-Delmotte, V., Stievenard, M., Hoffmann, G., Pierre, M., … Guibal, F. (2011). Can climate variations be inferred from tree-ring parameters and stable isotopes from *Larix decidua*? Juvenile effects, budmoth outbreaks, and divergence issue. *Earth and Planetary Science Letters*, *309*, 221–233. https://doi.org/10.1016/j.epsl.2011.07.003

Deslauriers, A., Beaulieu, M., Balducci, L., Giovannelli, A., Gagnon, M. J., & Rossi, S. (2014). Impact of warming and drought on carbon balance related to wood formation in black spruce. *Annals of Botany*, *114*(2), 335–345. https://doi.org/10.1093/aob/mcu111

Durbin, J., & Watson, G. S. (1971). Testing for serial correlation in least squares regression. III. *Biometrika*, *58*(1), 1–19. https://doi.org/10.1093/biomet/38.1-2.159

Esper, J., Frank, D., Büntgen, U., Verstege, A., Hantemirov, R., & Kirdyanov, A. V. (2010). Trends and uncertainties in Siberian indicators of 20th century warming. *Global Change Biology*, *16*, 386–398. https://doi.org/10.1111/j.1365-2486.2009.01913.x%20Trends

Falvey, M., & Garreaud, D. (2009). Regional cooling in a warming world: Recent temperature trends in the southeast Pacific and along the west coast of subtropical South America (1979–2006). *Journal of Geophysical Research*, *114*, D04102. https://doi.org/10.1029/2008JD010519

Farquhar, G. D., Ehleringer, J. R., & Hubick, K. T. (1989). Carbon isotope discrimination and photosynthesis. *Annual Review of Plant Physiology and Plant Molecular Biology*, *40*, 503–537. https://doi.org/10.1146/annurev.pp.40.060189.002443

Farquhar, G. D., Learyb, M. H. O., & Berry, J. A. (1982). On the relationship between carbon isotope discrimination and the intercellular carbon dioxide concentration in leaves. *Carbon*, *9*, 121–137.

Farquhar, G. D., & Richards, R. A. (1984). Isotopic composition of plant carbon correlates with water-use efficiency of wheat genotypes. *Australian Journal of Plant Physiology*, *11*, 539–552.

Frank, D. C., Poulter, B., Saurer, M., Esper, J., Huntingford, C., Helle, G., … Weigl, M. (2015). Water-use efficiency and transpiration across European forests during the Anthropocene. *Nature Climate Change*, *5*(6), 579–583. https://doi.org/10.1038/nclimate2614

Fritts, H. C. (1976). *Tree Rings and Climate*. London: *Academic Press*.

Garreaud, R., Lopez, P., Minvielle, M., & Rojas, M. (2013). Large-scale control on the Patagonian climate. *Journal of Climate*, *26*, 215–230. https://doi.org/10.1175/JCLI-D-12-00001.1

Gennaretti, F., Huard, D., Naulier, M., Savard, M., Bégin, C., Arseneault, D., & Guiot, J. (2017). Bayesian multiproxy temperature reconstruction with black spruce ring widths and stable isotopes from the northern Quebec taiga. *Climate Dynamics*, 123456789, 1–13. https://doi.org/10.1007/s00382-017-3565-5

Girardin, M. P., Bernier, P. Y., Raulier, F., Tardif, J. C., Conciatori, F., & Guo, X. J. (2011). Testing for a $CO_2$ fertilization effect on growth of Canadian boreal forests. *Journal of Geophysical Research*, *116*, G01012. https://doi.org/10.1029/2010JG001287

Girardin, M. P., Bouriaud, O., Hogg, E. H., Kurz, W., Zimmermann, N. E., Metsaranta, J. M., … Bhatti, J. (2016). No growth stimulation of Canada's boreal forest under half-century of combined warming and $CO_2$ fertilization. *Proceedings of the National Academy of Sciences*, *113*(52), 1–9. https://doi.org/10.1073/pnas.1610156113

Girardin, M. P., Hogg, E. H., Bernier, P. Y., Kurz, W. A., Guo, X. J., & Cyr, G. (2016). Negative impacts of high temperatures on growth of black spruce forests intensify with the anticipated climate warming. *Global Change Biology*, *22*(2), 627–643. https://doi.org/10.1111/gcb.13072

Hilasvuori, E., Berninger, F., Sonninen, E., Tuomenvirta, H., & Jungner, H. (2009). Stability of climate signal in carbon and oxygen isotope records and ring width from Scots pine (*Pinus sylvestris* L.) in Finland. *Journal of Quaternary Science*, *24*, 469–480. https://doi.org/10.1002/jqs.1260

Holmes, R. L. (1983). Computer-assisted quality control in tree-ring dating and measurement. *Tree-Ring Bulletin*, *43*(1), 69–78.

Huang, J.-G., Bergeron, Y., Denneler, B., Berninger, F., & Tardif, J. (2007). Response of forest trees to increased atmospheric $CO_2$. *Critical Reviews in Plant Sciences*, *26*, 265–283. https://doi.org/10.1080/07352680701626978

Intergovernmental Panel on Climate Change (2013). Climate Change 2013: The Physical Science Basis. In T. F. Stocker (Eds.), *Contribution of Working Group I to the Fifth Assessment Report of the Intergovernmental Panel on Climate Change* (1535 pp.) Cambridge, United Kingdom and New York, NY: Cambridge University Press. https://doi.org/10.1017/CBO9781107415324

Keeling, C. D. (1979). The Suess effect: $^{13}$Carbon–$^{14}$carbon interrelations. *Environment International*, *2*(4), 229–300.

Keeling, C. D., Piper, S. C., Bacastow, R. B., Wahlen, M., Whorf, T. P., Heimann, M., & Meijer, H. A. (2005). Atmospheric $CO_2$ and $^{13}CO_2$ exchange with the terrestrial biosphere and oceans from 1978 to 2000: Observations and carbon cycle implications. In J. R. Ehleringer, T. E. Cerling, & M. D. Dearing (Eds.), *A History of Atmospheric $CO_2$ and its effects on plants, animals, and ecosystems*, (pp. 83–113). New York: Springer Verlag.

Labuhn, I., Daux, V., Girardclos, O., Stievenard, M., Pierre, M., Chrono-environnement, L., … Masson-Delmotte, V. (2016). French summer droughts since 1326 CE: A reconstruction based on tree ring cellulose $\delta^{18}O$. *Climate of the Past*, *12*(6), 1101–1117. https://doi.org/10.5194/cp-12-1101-2016

Lara, A., & Villalba, R. (1993). A 3620-year temperature record from *Fitzroya cupressoides* tree rings in southern South America. *Science*, *260*, 1104–1106. https://doi.org/10.1126/science.260.5111.1104

Lara, A., & Villalba, R. (1994). Potencialidad de *Fitzroya cupressoides* para reconstrucciones climáticas durante el Holoceno en Chile y Argentina. *Revista Chilena de Historia Natural*, *67*, 443–451.
Lavergne, A. (2016). *Evaluation of Tree-Ring Archive as Paleoclimatic Tracer in Northern Patagonia*. France: Université Versailles Saint-Quentin.
Lavergne, A., Daux, V., Villalba, R., & Barichivich, J. (2015). Temporal changes in climatic limitation of tree-growth at upper treeline forests: Contrasted responses along the west-to-east humidity gradient in Northern Patagonia. *Dendrochronologia*, *36*, 49–59. https://doi.org/10.1016/j.dendro.2015.09.001
Lavergne, A., Daux, V., Villalba, R., Pierre, M., Stievenard, M., & Srur, A. M. (2017). Improvement of isotope-based climate reconstructions in Patagonia through a better understanding of climate influences on isotopic fractionation in tree rings. *Earth and Planetary Science Letters*, *459*, 372–380. https://doi.org/10.1016/j.epsl.2016.11.045
Lavergne, A., Daux, V., Villalba, R., Pierre, M., Stievenard, M., Srur, A. M., & Vimeux, F. (2016). Are the $\delta^{18}O$ of *F. cupressoides* and *N. pumilio* promising proxies for climate reconstructions in northern Patagonia? *Journal of Geophysical Research: Biogeosciences*, *121*, 767–776. https://doi.org/10.1002/2015JG003260
Leavitt, S. W., & Danzer, S. R. (1993). Method for batch processing small wood samples to holocellulose for stable-carbon isotope analysis. *Analytical Chemistry*, *65*(1), 87–89.
Lévesque, M., Siegwolf, R., Saurer, M., Eilmann, B., & Rigling, A. (2014). Increased water-use efficiency does not lead to enhanced tree growth under xeric and mesic conditions. *New Phytologist*, *203*(1), 94–109. https://doi.org/10.1111/nph.12772
Li, J., Xie, S.-P., Cook, E. R., Morales, M. S., Christie, D. A., Johnson, N. C., … Fang, K. (2013). El Niño modulations over the past seven centuries. *Nature Climate Change*, *3*(9), 822–826. https://doi.org/10.1038/nclimate1936
Linares, J. C., & Camarero, J. J. (2011). Growth patterns and sensitivity to climate predict silver fir decline in the Spanish Pyrenees. *European Journal of Forest Research*, *131*, 1001–1012. https://doi.org/10.1007/s10342-011-0572-7
Linares, J. C., & Camarero, J. J. (2012). From pattern to process: Linking intrinsic water-use efficiency to drought-induced forest decline. *Global Change Biology*, *18*, 1000–1015. https://doi.org/10.1111/j.1365-2486.2011.02566.x
Mantua, N. J., & Hare, S. R. (2002). The Pacific Decadal Oscillation. *Journal of Oceanography*, *58*, 35–44. https://doi.org/10.1023/A:1015820616384
Mantua, N. J., Hare, S. R., Zhang, Y., Wallace, J. M., & Francis, R. C. (1997). A Pacific interdecadal climate oscillation with impacts on salmon production. *Bulletin of the American Meteorological Society*, *78*(6), 1069–1079. https://doi.org/10.1175/1520
Markgraf, V., & Diaz, H. (2000). The past ENSO record: A synthesis. In *El Niño and the Southern Oscillation: Multiscale Variability and Global and Regional Impacts*, (pp. 478–479). Cambridge, UK: Cambridge University Press.
Marshall, G. J. (2003). Trends in the Southern Annular Mode from observations and reanalyses. *Journal of Climate*, *16*, 4134–4143.
McCarroll, D., & Loader, N. J. (2004). Stable isotopes in tree rings. *Quaternary Science Reviews*, *23*, 771–801.
McDowell, N. G., Beerling, D. J., Breshears, D. D., Fisher, R. A., Raffa, K. F., & Stitt, M. (2011). The interdependence of mechanisms underlying climate-driven vegetation mortality. *Trends in Ecology & Evolution*, *26*, 523–532. https://doi.org/10.1016/j.tree.2011.06.003
Melvin, T. M., & Briffa, K. R. (2008). A "signal-free" approach to dendroclimatic standardisation. *Dendrochronologia*, *26*(2), 71–86.
Melvin, T. M., & Briffa, K. R. (2014). CRUST: Software for the implementation of Regional Chronology Standardisation: Part 1. Signal-free RCS. *Dendrochronologia*, *32*(1), 7–20. Retrieved from. https://doi.org/10.1016/j.dendro.2013.06.002
Naulier, M., Savard, M. M., Bégin, C., Marion, J., Nicault, A., & Bégin, Y. (2015). Temporal instability of isotopes–climate statistical relationships—A study of black spruce trees in northeastern Canada. *Dendrochronologia*, *34*, 33–42. https://doi.org/10.1016/j.dendro.2015.04.001
Neira, E., & Lara, A. (2000). Desarrollo de cronologia de ancho de anillos para alerce. *Revista Chilena de Historia Natural*, *73*, 693–703.
Neukom, R., Gergis, J., Karoly, D. J., Wanner, H., Curran, M., Elbert, J., … Frank, D. (2014). Inter-hemispheric temperature variability over the past millennium. *Nature Climate Change*, *4*(5), 362–367. https://doi.org/10.1038/nclimate2174
Norby, R., Wullschleger, S. D., & Gunderson, C. (1999). Tree responses to rising $CO_2$ in field experiments: Implications for the future forest. *Plant, Cell and Environment*, *22*, 683–714.
Norby, R. J., Warren, J. M., Iversen, C. M., Medlyn, B. E., & McMurtrie, R. E. (2010). $CO_2$ enhancement of forest productivity constrained by limited nitrogen availability. *Proceedings of the National Academy of Sciences of the United States of America*, *107*, 19,368–19,373. https://doi.org/10.1073/pnas.1006463107
Peñuelas, J., Canadell, J. G., & Ogaya, R. (2011). Increased water-use efficiency during the 20th century did not translate into enhanced tree growth. *Global Ecology and Biogeography*, *20*, 597–608. https://doi.org/10.1111/j.1466-8238.2010.00608.x
Pettitt, A. N. (1979). A non-parametric approach to the change point problem. *Journal of the Royal Statistical Society: Series C: Applied Statistics*, *28*, 126–135.
Prentice, I. C., & Harrison, S. P. (2009). Ecosystem effects of $CO_2$ concentration: Evidence from past climates. *Climate of the Past*, *5*, 937–963. https://doi.org/10.5194/cpd-5-937-2009
Raczka, B., Duarte, H. F., Koven, C. D., Ricciuto, D., Thornton, P. E., Lin, J. C., & Bowling, D. R. (2016). An observational constraint on stomatal function in forests: Evaluating coupled carbon and water vapor exchange with carbon isotopes in the Community Land Model (CLM4.5). *Biogeosciences*, *13*(18), 5183–5204. https://doi.org/10.5194/bg-13-5183-2016
Reynolds-Henne, C. E., Siegwolf, R. T. W., Treydte, K. S., Esper, J., Henne, S., & Saurer, M. (2007). Temporal stability of climate–isotope relationships in tree rings of oak and pine (Ticino, Switzerland). *Global Biogeochemical Cycles*, *21*, GB4009. https://doi.org/10.1029/2007GB002945
Rodríguez-Catón, M., Villalba, R., Morales, M., & Srur, A. (2016). Influence of droughts on *Nothofagus pumilio* forest decline across northern Patagonia, Argentina. *Ecosphere*, *7*(7). https://doi.org/10.1002/ecs2.1390
Salzer, M. W., Hughes, M. K., Bunn, A. G., & Kipfmueller, K. F. (2009). Recent unprecedented tree-ring growth in bristlecone pine at the highest elevations and possible causes. *Proceedings of the National Academy of Sciences of the United States of America*, *106*, 20,348–20,353. https://doi.org/10.1073/pnas.0903029106
Seftigen, K., Linderholm, H. W., Loader, N. J., Liu, Y., & Young, G. H. F. (2011). The influence of climate on $^{13}C/^{12}C$ and $^{18}O/^{16}O$ ratios in tree ring cellulose of *Pinus sylvestris* L. growing in the central Scandinavian mountains. *Chemical Geology*, *286*, 84–93. https://doi.org/10.1016/j.chemgeo.2011.04.006
Silva, L. C. R., Anand, M., & Leithead, M. D. (2010). Recent widespread tree growth decline despite increasing atmospheric $CO_2$. *PLoS One*, *5*. https://doi.org/10.1371/journal.pone.0011543
Silva, L. C. R., & Madhur, A. (2013). Probing for the influence of atmospheric $CO_2$ and climate change on forest ecosystems across biomes. *Global Ecology and Biogeography*, *22*(1), 83–92. https://doi.org/10.1111/j.1466-8238.2012.00783.x
Stokes, M. A., & Smiley, T. L. (1968). *An Introduction to Tree-Ring Dating*. Chicago: The University of Chicago Press.
Trenberth, K. E., & Hurrell, J. W. (1994). Decadal atmosphere–ocean variations in the Pacific. *Climate Dynamics*, *9*(6), 303–319. https://doi.org/10.1007/BF00204745

Urrutia-Jalabert, R., Malhi, Y., Barichivich, J., & Lara, A. (2015). Increased water use efficiency but contrasting tree growth patterns in *Fitzroya cupressoides* forests of southern Chile during recent decades. *Journal of Geophysical Research: Biogeosciences*, *120*, 2505–2524. https://doi.org/10.1002/2015JG003098

Urrutia-Jalabert, R., Malhi, Y., & Lara, A. (2015). The oldest, slowest rainforests in the world? Massive biomass and slow carbon dynamics of *Fitzroya cupressoides* temperate forests in southern Chile. *PLoS One*, *10*(9), 1–24. https://doi.org/10.1371/journal.pone.0137569

Urrutia-Jalabert, R., Rossi, S., Deslauriers, A., Malhi, Y., & Lara, A. (2015). Environmental correlates of stem radius change in the endangered *Fitzroya cupressoides* forests of southern Chile. *Agricultural and Forest Meteorology*, *200*, 209–221. https://doi.org/10.1016/j.agrformet.2014.10.001

Villalba, R. (1990). Climatic fluctuations in northern Patagonia during the last 1000 years as inferred from tree-ring records. *Quaternary Research*, *34*, 346–360.

Villalba, R., Grosjean, M., & Kiefer, T. (2009). Long-term multi-proxy climate reconstructions and dynamics in South America (LOTRED-SA): State of the art and perspectives. *Palaeogeography, Palaeoclimatology, Palaeoecology*, *281*, 175–179.

Villalba, R., Lara, A., Boninsegna, J. A., Masiokas, M., Delgado, S., Aravena, J. C., … Ripalta, A. (2003). Large-scale temperature changes accross the Southern Andes: 20th-century variations in the context of the past 400 years. *Climatic Change*, *59*, 177–232.

Villalba, R., Lara, A., Masiokas, M. H., Urrutia, R. R., Luckman, B. H., Marshall, G. J., … LeQuesne, C. (2012). Unusual Southern Hemisphere tree growth patterns induced by changes in the Southern Annular Mode. *Nature Geoscience*, *5*, 793–798. https://doi.org/10.1038/ngeo1613

Voelker, S. L., Brooks, J. R., Meinzer, F. C., Anderson, R., Bader, M. K.-F., Battipaglia, G., … Wingate, L. (2015). A dynamic leaf gas-exchange strategy is conserved in woody plants under changing ambient $CO_2$: Evidence from carbon isotope discrimination in paleo and $CO_2$ enrichment studies. *Global Change Biology*, *22*(2), 889–902. https://doi.org/10.1111/gcb.13102

Wang, X. Z. (2007). Effects of species richness and elevated carbon dioxide on biomass accumulation: A synthesis using meta-analysis. *Oecologia*, *152*(4), 595–605. https://doi.org/10.1007/s00442-007-0691-5

Wigley, T. M. L., Briffa, K. R., & Jones, P. D. (1984). On the average value of correlated time series, with applications in dendroclimatology and hydrometeorology. *Journal of Climate and Applied Meteorology*, *23*(2), 201–213.

Wilson, R., Anchukaitis, K., Briffa, K. R., Büntgen, U., Cook, E., D'Arrigo, R., … Zorita, E. (2016). Last millennium Northern Hemisphere summer temperatures from tree rings: Part I: The long term context. *Quaternary Science Reviews*, *134*, 1–18. https://doi.org/10.1016/j.quascirev.2015.12.005

Wolkovich, E. M., Cook, B. I., Allen, J. M., Crimmins, T. M., Betancourt, J. L., Travers, S. E., … Cleland, E. E. (2012). Warming experiments underpredict plant phenological responses to climate change. *Nature*, *485*(7399), 18–21. https://doi.org/10.1038/nature11014

Young, G. H. F., Demmler, J. C., Gunnarson, B. E., Kirchhefer, A. J., Loader, N. J., & McCarroll, D. (2011). Age trends in tree ring growth and isotopic archives: A case study of *Pinus sylvestris* L. from northwestern Norway. *Global Biogeochemical Cycles*, *25*, GB2020. https://doi.org/10.1029/2010GB003913

Zang, C., & Biondi, F. (2015). treeclim: an R package for the numerical calibration of proxy–climate relationships. *Ecography*, *38*(4), 431–436. https://doi.org/10.1111/ecog.01335